INTERNATIONAL
ATOMIC ENERGY
AGENCY

UNITED NATIONS
EDUCATIONAL,
SCIENTIFIC
AND CULTURAL
ORGANIZATION

LAMP/91/10

INTERNATIONAL CENTRE FOR
THEORETICAL PHYSICS

LAMP
SERIES REPORT

(Laser, Atomic and Molecular Physics)

RIGID NOTATIONS IN TWO-ELECTRON ATOMS IN A UNIFORM MAGNETIC FIELD

J. Mahecha G.

MIRAMARE-TRIESTE

Preface

The ICTP-LAMP reports consist of manuscripts relevant to seminars and discussions held at ICTP in the field of Laser, Atomic and Molecular Physics (LAMP).

These reports aim at informing LAMP researchers on the activity carried out at ICTP in their field of interest, with the specific purpose of stimulating scientific contacts and collaboration of physicists from Third World Countries.

If you are interested in receiving additional information on the Laser and Optical Fibre activities at ICTP, kindly contact Professor Gallieno Denardo, ICTP.

International Atomic Energy Agency
and
United Nations Educational Scientific and Cultural Organization
INTERNATIONAL CENTRE FOR THEORETICAL PHYSICS

LAMP SERIES REPORT

(Laser, Atomic and Molecular Physics)

RIGID ROTATIONS IN TWO–ELECTRONS ATOMS IN A UNIFORM MAGNETIC FIELD

J. Mahecha G. *
International Centre for Theoretical Physics, Trieste, Italy.

ABSTRACT

Two exact rigid body solutions for a rotating two–electron atom under the influence of a magnetic field directed along the rotation axis were obtained using a classical approach. A solution gives at zero field the same result previously known as a rigid rotor. The other solution at zero field gives the previous result known as an asymmetric top or Langmuir solution. A stability analysis of the linearized motions near each of these equilibrium motions was made for different values of the magnetic field intensity. It was found that they are unstable but can exist during certain time for certain combinations of the magnetic field intensity and the angular momentum. The experimental realization of these classical states are the resonant states which would manifest in the spectrum as a subset of the quasi–Landau resonances. An examination of the energy levels near the ionization threshold shows that, in fact, they are similar to the quasi–Landau resonances. Also analytical expressions for the diamagnetic susceptibility of the two–excited states reported in this work were found. For the purpose of comparison, a study of the classical diamagnetism in one–electron atoms is presented.

MIRAMARE – TRIESTE
December 1991

* Permanent address: Departamento de Física, Universidad de Antioquia, A.A. 1126, Medellín, Colombia.

1. Introduction

During last few years several classical and semiclassical studies about the resonant states which occur in the double excitations of two-electron atomic systems (Klar 1986a, 1986b, 1986c) together with stability analysis were made (Klar 1986a, 1987a, 1987b). Various authors had been interested in this kind of classical calculations before (Langmuir 1921, Dimitrijević and Grujić 1984, Wannier 1953, Poirier 1989), specially considering double excitations in free two-electron atoms. Earlier I reported also results referring to double excited states under the effect of electric fields (Mahecha 1989). This kind of calculations had shown two types of correlated motions of the excited electronic pair. In the first one the electrons and the nucleus form a linear configuration similar to CO_2 molecule which for brevity will be named "electronic rotor". In the second configuration the electrons rotate around circular orbits on parallel planes with the nucleus and the electrons forming a rigid triangular structure. This configuration will be named "electronic top". As is well known, in these states the electrons have a highly correlated motion and for this reason a description based on a central field model using independent coordinates fails (Fano 1983).

It has been found that a convenient coordinate system to describe this kind of systems is the hyperspherical set. In the current literature two types of such coordinate systems are used. One introduced by Fock (Fock 1958), and used by Fano and others (Fano 1983), is based on the replacement of the electron-nucleus distances r_1 and r_2 by the hyperradius $r = (r_1^2 + r_2^2)^{1/2}$ and the mock angle $\alpha = \tan^{-1}(r_2/r_1)$, leaving as remaining coordinates the usual ones $\theta_1, \phi_1, \theta_2$ and ϕ_2. In this article we will employ a different system, introduced by Smith (Smith 1962) and used by Klar and others, in which the electrons, in a rotating frame, are specified by two mock angles ϕ and ψ and the hyperradius r, and the rotating frame is located with respect to the space axes with the help of the Euler angles α, β and γ (Klar 1985). In the equilibrium motions only the angle α describing the overall rotation of the atom is a time dependent coordinate.

Most of the double excited states of He and other two electron systems are autoionizing, as predicted by simple classical models. A rigorous stability of the rotating atom, in the Liapunov sense, is not expected. However, the spectrum of characteristic Liapunov exponents gives information about the local nature of the equilibrium states (Berry 1983, Abraham and Marsden 1978). In the present work the corresponding calculations when the atom is under the effect of a homogeneous magnetic field are presented.

It is important to study the Zeeman effect in two-electron excited systems with correlated motion. There are many works about one-electron atoms under external magnetic fields (Wuner and Ruder 1987, Delande *et al* 1984), and some efforts toward the comprehension of the chaotic behavior of hydrogenoid atoms in magnetic fields (Wintgen and Friedrich 1987). Also there are numerical calculations about electron trajectories in a hydrogen atom under a magnetic field, and semiclassical calculations, WKB, of the quasi-Landau

resonances in this system (Delos *et al* 1983, Delos *et al* 1984, Gallas and O'Connell 1982). However, there are few works in the literature about highly excited two-electron atoms in the presence of magnetic fields. In the present work, we solve one of the simplest problems involving two-electron atoms under magnetic fields of arbitrary intensity. The present investigation can be also relevant to the study of bound matter-antimatter systems, such as $\bar{p}e^+e^+$, for the spectroscopy of two-electron Rydberg atoms in a magnetic trap, and for the spectroscopy of neutron stars or white dwarf in which the atoms are under enormous magnetic fields.

The paper is organized as follows. In sections 2 and 3 an introduction to the mathematical description of the system is given. In section 4 two exact analytical solutions found in this study are presented. In section 5 a stability analysis is given. In section 6 the calculation of the magnetic susceptibility is presented and the connection with quasi-Landau resonances is analyzed, and in section 7 a discussion of our results is presented. We use atomic units and the notations of the references (Klar 1986a,b,c, Klar 1987a,b), and an infinite value for the nuclear mass is assumed. An atomic unit of the magnetic field has the value $2.35 \times 10^9 G$. In order to be specific, we refer the numerical results to the H^- ion with angular momentum $L_z = 1$.

2. Classical Equations of Motion. Lagrangian Formulation

The kinetic and potential energies of the free system are,

$$T = \frac{1}{2}(\dot{\vec{r}}_1^{\,2} + \dot{\vec{r}}_2^{\,2}), \qquad V = -\frac{Z}{r_1} - \frac{Z}{r_2} + \frac{1}{r_{12}}. \tag{1}$$

The magnetic forces can be obtained from the following velocity dependent potential,

$$V_H = \vec{A}(\vec{r}_1).\dot{\vec{r}}_1 + \vec{A}(\vec{r}_2).\dot{\vec{r}}_2, \tag{2}$$

where $\vec{A}(\vec{r})$ is the vector potential, in this case generated by a homogeneous magnetic field along the z axis, $\vec{H} = H\vec{k}$, which with certain gauge selection has the form

$$\vec{A}(\vec{r}) = \frac{1}{2}(x\vec{j} - y\vec{i})\,H. \tag{3}$$

It is convenient to define a set (q) of six coordinates

$$q_1 = \alpha, \quad q_2 = \beta, \quad q_3 = \gamma, \quad q_4 = r, \quad q_5 = \psi, \quad q_6 = \phi, \tag{4}$$

where α, β and γ are Euler angles and r, ψ and ϕ are hyperspherical coordinates. The transformation from the cartesian to the hyperspherical coordinates is

$$\vec{r}_i = \underset{\sim}{R}(-\alpha, -\beta, -\gamma)\,\vec{\rho}_i, \quad i = 1, 2, \tag{5}$$

where $\underset{\sim}{R}$ is the rotation matrix, and the internal coordinates $\vec{\rho}_i$, expressed in the hyperspherical coordinates, are given by (Klar 1986a,b,c, Klar 1987a,b, Klar 1985)

$$\vec{\rho}_{1,2} = r \begin{pmatrix} \cos\psi \cos(\phi/2 \pm 3\pi/4) \\ \sin\psi \sin(\phi/2 \pm 3\pi/4) \\ 0 \end{pmatrix}, \tag{6}$$

where $0 \le \psi \le \pi/4$, $0 \le \phi \le 2\pi$.

One can express T, V and V_H in terms of these coordinates in order to obtain the Lagrangian. T consists of the internal, rotational and Coriolis contributions,

$$T = T_{int} + T_{rot} + T_{cor}, \tag{7}$$

$$T_{int} = \frac{1}{2}\dot{r}^2 + \frac{1}{2}r^2\dot{\psi}^2 + \frac{1}{8}r^2\dot{\phi}^2, \tag{8}$$

$$T_{rot} = \frac{1}{8}r^2\dot{\alpha}^2[3 + \cos 2\beta + (1 - \cos 2\beta)\cos 2\psi \cos 2\gamma] + \frac{1}{4}r^2\dot{\beta}^2(1 - \cos 2\psi \cos 2\gamma) + \frac{1}{2}r^2\dot{\gamma}^2 - \frac{1}{2}r^2\dot{\alpha}\dot{\beta}\sin\beta \sin 2\gamma \cos 2\psi + r^2\dot{\alpha}\dot{\gamma}\cos\beta, \tag{9}$$

$$T_{cor} = \frac{1}{2}r^2\dot{\alpha}\dot{\phi}\cos\beta \sin 2\psi + \frac{1}{2}r^2\dot{\gamma}\dot{\phi}\sin 2\psi. \tag{10}$$

The potential energy depends on the Coloumb interactions and on the velocity dependent magnetic interactions.

The Coulomb term has the expression,

$$V = \frac{1}{r}C(\psi, \phi), \tag{11}$$

where the function C is given by (Klar 1986,a,b,c, Klar 1987a,b)

$$C(\psi, \phi) = -Z\,2^{1/2}[(1 + \cos 2\psi \sin\phi)^{-1/2} + (1 - \cos 2\psi \sin\phi)^{-1/2}] + (1 - \cos 2\psi \cos\phi)^{-1/2}. \tag{12}$$

And the magnetic potential energy V_H takes the following expression in the hyperspherical variables,

$$V_H = \frac{H}{8}\dot{\alpha}r^2[3 + \cos 2\beta + (1 - \cos 2\beta)\cos 2\psi \cos 2\gamma] - \frac{H}{4}\dot{\beta}r^2 \cos 2\psi \sin 2\gamma \sin\beta + \frac{H}{2}\dot{\gamma}\cos\beta r^2 + \frac{H}{4}\dot{\phi}r^2 \cos\beta \sin 2\psi. \tag{13}$$

Now the Lagrangian equations of the motion in terms of the variables (q) and $(\dot{q})$ can be written. As far as the Euler angle α is a cyclic coordinate, the Lagrangian equation with respect to α gives the conserved angular momentum L_z. Another constant of the motion is the total energy E (which in this case is not simply $T + V$). An explicit form of the Lagrangian equations for the free system is given in the reference (Klar 1987b). In the present problem, each equation will have field dependent terms. The complete expression for the differential equations of motion has many terms. Since we are only interested in the equilibrium motions, it is enough to find the algebraic system of equations resulting when the following rigidity and rotational equilibrium conditions to the equations of the motion are applied

$$\dot{r} = \dot{\psi} = \dot{\phi} = 0, \quad \dot{\alpha} = \omega, \quad \dot{\beta} = \dot{\gamma} = 0, \tag{14}$$

with the use of which the following system of 6 non linear algebraic equations is obtained

$$L_z = \frac{1}{8}r^2(2\omega - H)[3 + \cos 2\beta + (1 - \cos 2\beta)\cos 2\psi \cos 2\gamma], \tag{15}$$

$$0 = (-4\omega^2 + H^2)r^2 \sin 2\beta(-1 + \cos 2\psi \cos 2\gamma), \tag{16}$$

$$0 = (-4\omega^2 + H^2)r^2(\cos 2\beta - 1)\cos 2\psi \sin 2\gamma, \tag{17}$$

$$0 = \frac{1}{16}(-4\omega^2 + H^2)r[3 + \cos 2\beta + (1 - \cos 2\beta)\cos 2\psi \cos 2\gamma] - \frac{C}{r^2}, \tag{18}$$

$$0 = \frac{1}{16}(-4\omega^2 + H^2)r^2(-1 + \cos 2\beta)\sin 2\psi \cos 2\gamma - \frac{1}{r}\frac{\partial C}{\partial \psi}, \tag{19}$$

$$0 = \frac{1}{r}\frac{\partial C}{\partial \phi}. \tag{20}$$

Equation (15) permits replacing the angular velocity ω by the conserved angular momentum L_z.

3. Classical Equations of Motion. Routhian Formulation

Insofar as the system has a cyclic variable and the potential energy depends on the generalized velocities, it is convenient to formulate the problem with a lower number of variables.

The Lagrangian constructed from (7-13) has the form,

$$L = \frac{1}{2}M_{\mu\nu}(q)\dot{q}_\mu\dot{q}_\nu - V(q) - R_\mu(q)\dot{q}_\mu, \tag{21}$$

where the sum convention, for $\mu, \nu = 1, 2, \ldots 6$, has been used. Note that the coordinate α neither appears in $M_{\mu\nu}$ nor in V.

The components of the 6-dimensional vector R_μ are given by

$$R_\mu = \frac{1}{2} H M_{1\mu}, \quad \mu = 1, 2, ...6. \tag{22}$$

It is not useful to construct the corresponding Hamiltonian to describe a flux in a 12-dimensional phase space because the matrix $\underset{\sim}{M}$ is singular when it is evaluated at equilibrium and we are precisely interested in the linearized motion near the equilibrium configurations.

In order to analyze the phase space motion, it is convenient to eliminate the subspace corresponding to the cyclic coordinate α, by expressing the angular frequency of rotation $\omega = \dot{\alpha}$ as a function of the conserved angular momentum L_z. This can be done in an easy and elegant way in the Routh formalism (Whittaker 1937, Abraham and Marsden 1978), which allows reducing the dimension of the problem according to the number of cyclic coordinates, leaving as parameters the constant values of their canonically conjugate momenta, in our case L_z (Whittaker 1937, Abraham and Marsden 1978). In this formulation the reduced problem will have five generalized coordinates which we will redefine as $(q) = (\beta, \gamma, r, \psi, \phi)$.

The conserved angular momentum in the Lagrangian formulation is,

$$L_z = \frac{\partial L}{\partial \dot{\alpha}} = (\dot{\alpha} - \frac{1}{2} H) M_{11} + M_{1\mu} \dot{q}_\mu. \tag{23}$$

In the following discussions we will use the reduced coordinates, with which $\mu = 2, 3, ...6$. In consequence, the Routhian function of the system is

$$-R = \frac{1}{2} M^*_{\mu\nu} \dot{q}_\mu \dot{q}_\nu - \frac{(L_z + R_1)^2}{2 M_{11}} + K_\mu \dot{q}_\mu - V, \tag{24}$$

where now the problem instead of a six-dimensional matrix $\underset{\sim}{M}$ will have a five-dimensional matrix $\underset{\sim}{M}^*$ and a vector $\vec{K}$, defined by

$$M^*_{\mu\nu} = M_{\mu\nu} - \frac{M_{1\mu} M_{1\nu}}{M_{11}}, \tag{25}$$

$$K_\mu = \frac{L_z M_{1\mu}}{M_{11}}. \tag{26}$$

It is simple to verify that the equilibrium equations (16)-(20) are equivalent to

$$\frac{\partial}{\partial q_\mu} \left(\frac{(L_z + R_1)^2}{2 M_{11}} + V \right) = 0. \tag{27}$$

As far as $det\ \underset{\sim}{M}^* \neq 0$, we can calculate the reduced Hamiltonian Q corresponding to $-R$. This can be done with the help of $\underset{\sim}{N}^*$ which is the inverse matrix of $\underset{\sim}{M}^*$. The result is,

$$Q = \frac{1}{2} N^*_{\mu\nu} (p_\mu - K_\mu)(p_\nu - K_\nu) + \frac{(L_z + R_1)^2}{2 M_{11}} + V. \tag{28}$$

In consequence, the expression for the total energy in the equilibrium is given by the effective potential energy $(L_z + R_1)^2/2M_{11} + V$ evaluated at equilibrium, which can have any of the following forms

$$\begin{aligned} E &= \frac{1}{8} (2\omega + H)^2 M_{11} + \frac{1}{r} C, \\ &= \frac{1}{2} H L_z + \frac{L_z^2}{2 M_{11}} + \frac{1}{8} H^2 M_{11} + \frac{1}{r} C, \end{aligned} \tag{29}$$

and M_{11} has the expression

$$M_{11} = \frac{1}{4} r^2 [3 + \cos 2\beta + (1 - \cos 2\beta) \cos 2\psi \cos 2\gamma]. \tag{30}$$

$L_z^2/2M_{11}$ is a centrifugal term. $HL_z/2$ is the normal Zeeman effect term which would be omitted without drastically changing the results. The non trivial effects are contained in the diamagnetic term, $H^2 M_{11}/8$.

4. Classical Equilibrium Equations

The system of equations (16)-(20) admits two types of solutions. One corresponds to the "electronic top"

$$\beta = \frac{\pi}{2}, \quad \gamma = 0, \quad r = r_0, \quad \psi = \psi_0, \quad \phi = 0, \tag{31}$$

where r_0 is solution to the equation

$$H^2 r^4 + 8\sqrt{2} Z r - \frac{4 L_z^2}{k^4} = 0, \tag{32}$$

and ψ_0 is related with k and Z by

$$\cos \psi_0 = k = [1 - (4Z)^{-2/3}]^{1/2}. \tag{33}$$

$\beta = \pi/2$ means that the electrons remain in a plane containing the rotation axis, as is shown in figure 1a. The semiclassical distribution of probabilities in this state is zero on the rotation axis and in the neighborhoods of a plane which contains the nucleus, perpendicular to the field, and it is large on two planes which contain the classical orbits.

The energy at the equilibrium is given by Q, evaluated at equilibrium, equation (29)

$$E = \frac{L_z^2}{2\,k^2\,r_0^2} - \frac{2\sqrt{2}\,Z\,k^2}{r_0} + \frac{H\,L_z}{2} + \frac{H^2\,k^2\,r_0^2}{8}. \tag{34}$$

The other solution corresponds to the "electronic rotor"

$$\beta = \text{arbitrary}, \quad \gamma = 0, \quad r = r_0, \quad \psi = 0, \quad \phi = \pi, \tag{35}$$

where r_0 is solution to the equation

$$H^2 r^4 + 2\sqrt{2}(4\,Z - 1)\,r - 4\,L_z^2 = 0, \tag{36}$$

The "electronic rotor" equilibrium is degenerate and there exist an infinity of solutions for β angles between zero and π, all with equal energy and hyperradius, for given values of L_z and H. Since the β coordinate is not a good quantum number, it is expected that, as a result of the quantum effects, states are produced which are a superposition of the associated states corresponding to different values of β. The semiclassical probability distribution will have a great value near to a circle with radius r_0 located in the plane perpendicular to the field and containing the nucleus and gradually diminishes being zero on the rotation axis.

The energy at equilibrium is given by Q, evaluated at equilibrium, equation (29)

$$E = \frac{L_z^2}{2\,r_0^2} - \frac{4\,Z - 1}{\sqrt{2}\,r_0} + \frac{H\,L_z}{2} + \frac{H^2\,r_0^2}{8}. \tag{37}$$

In the two cases studied, the angular momentum is given respectively by

$$L_z = \frac{1}{2}\,r_0^2(2\,\omega - H)\cos^2\psi_0, \quad L_z = \frac{1}{2}\,r_0^2(2\,\omega - H). \tag{38}$$

Note that $L_z \leq 0$ when $\omega \leq H/2$. This means that negative values of L_z are not necessarily related with a counterclockwise rotation. The energy is different for different negative values of L_z, but in the Landau case (negligible Coulomb interactions in comparison with the magnetic one) the energy depends on $M + |M|$ with which all the states with $M \leq 0$ have equal energy as the state $M = 0$ (Delande *et al* 1984).

Typical electron configurations are represented in Figures 1a and 1b. Figures 2 show the hyperradius for each of the equilibria as a function of the field intensity. The shape of the triangle formed by the nucleus and the electrons, in the electronic top case, is conserved for all values of the field intensity, however, its size is reduced. When the angular momentum

is high it is observed that the atomic size is strongly diminished when the field intensity is increased.

The equation which determines r_0 is a fourth degree polynomial in r with coefficients depending on L_z^2, H^2 and Z. Then r is independent on the signs of L_z and H. Besides ψ_0 does not depend on H. In particular, in the top equilibrium the angle between the vectors $\vec{r}_1$ and $\vec{r}_2$ does not depend on the field. There is only a real, positive solution for each of the r_0 equations. It is possible to analytically solve the quartic equations for r and it is found that the problem has only one solution with a physical meaning, in each of the equilibria studied. The plot of the allowed solution as a function of H shows a maximum in $H = 0$ which significantly increases when the L_z value increases.

When the field is zero the earlier known result is obtained. Note that the form of the probability distributions associated with these states is similar for all values of the field intensity.

Figs.1a,1b

It can be verified that the force on each electron is zero for each of these configurations in the rotating frame,

$$\vec{F}_i = -\frac{Z}{r_i^3}\,\vec{\rho}_i + \frac{1}{r_{12}^3}(\vec{\rho}_i - \vec{\rho}_j) - \vec{\omega} \times (\vec{\omega} \times \vec{\rho}_i) + \vec{H} \times (\omega \times \vec{\rho}_i), \tag{39}$$

where $\vec{\omega}$ and $\vec{H}$ are vectors along the space axis z, and $\vec{\rho}_i$ are rigid body coordinates. We will choose the rotating axis to have the "x" and "y" components of the vectors $\vec{\rho}_i$ perpendicular to $\vec{\omega}$. In consequence, the equilibrium equations in the rotating frame only have "x" and "y" components,

$$-\frac{Z}{r_i^3}\,x_i + \frac{1}{r_{12}^3}(x_i - x_j) + \omega^2\,x_i - \omega\,H\,x_i = 0, \qquad -\frac{Z}{r_i^3}\,y_i + \frac{1}{r_{12}^3}(y_i - y_j) + \omega^2\,y_i - \omega\,H\,y_i = 0, \tag{40}$$

x_i, y_i are components of $\vec{\rho}_i$. Only the solutions of the system (16)-(20) consistent with (40) are to be accepted.

Figs.2a,2b

5. Stability of the Rigid Body Motions

The surface defined by the effective potential energy $(L_z+R_1)^2/2M_{11}+V$ has no points of minima, in contrast with the hydrogenoid case. It has some saddle points, as it is evident from the simple observation of the ten graphs $V_{ef}(q)$ with three coordinates evaluated at equilibrium. Such graphs have local maxima along the directions in which only one of the coordinates ϕ or β in the top case, and along ϕ in the rotor case, is changed, and minima along the remaining coordinates. This shows that values of the magnetic field or L_z for which the effective potential energy can bound the system do not exist, as can be verified by the analysis of the linearized motion in the neighborhood of the saddle points of V_{ef}.

According to equation (28), defining the reduced Hamiltonian Q, the Hamiltonian equations of the motion are,

$$\dot{p}_\mu = -\frac{1}{2}\frac{\partial N^*_{\nu\lambda}}{\partial q_\mu}(p_\nu - K_\nu)(p_\lambda - K_\lambda) + N^*_{\nu\eta}\frac{\partial K_\nu}{\partial q_\mu}(p_\eta - K_\eta) - \frac{\partial}{\partial q_\mu}\Big(\frac{(L_z+R_1)^2}{2M_{11}} + V\Big) \quad (41)$$

$$\dot{q}_\mu = N^*_{\mu\nu}(p_\nu - K_\nu). \quad (42)$$

Since $p_\mu = M^*_{\mu\nu}\dot{q}_\nu + K_\mu$ and the $M^*_{\mu\nu}$ are finite at equilibrium, we can see that the values of the momenta at equilibrium are given by

$$p^0_\mu = K_\mu(q^0), \quad (43)$$

where (q^0) is a solution of the equilibrium equations (16)-(20).

The reduced phase space is 10-dimensional in the top case and 8-dimensional in the rotor case. Its points are $\vec{x} = (\vec{q}-\vec{q}^0, \vec{p}-\vec{p}^0)$, with $\vec{q} = (\beta, \gamma, r, \psi, \phi)$, in the top case and $\vec{q} = (\gamma, r, \psi, \phi)$ in the rotor case, and $\vec{p}$ is their canonical conjugate momentum. If the equations of motion are linearized in the neighborhood of the equilibrium position in the reduced phase space, we obtain the equations of a dynamical system of the form $\dot{\vec{x}} = \underset{\sim}{\mathcal{M}}\,\vec{x}$, where the matrix $\underset{\sim}{\mathcal{M}}$, 10×10 or 8×8, is infinitesimally symplectic (Abraham and Marsden 1978), which implies that its eigenvalues are complex,

$$\begin{pmatrix}\dot{\vec{q}}\\ \dot{\vec{p}}\end{pmatrix} = \underset{\sim}{\mathcal{M}}\begin{pmatrix}\vec{q}-\vec{q}^0\\ \vec{p}-\vec{p}^0\end{pmatrix} = \begin{pmatrix} -\underset{\sim}{N}^*\underset{\sim}{A} & \underset{\sim}{N}^* \\ -\underset{\sim}{A}^T\underset{\sim}{N}^*\underset{\sim}{A} + \underset{\sim}{B} & \underset{\sim}{A}^T\underset{\sim}{N}^*\end{pmatrix}\begin{pmatrix}\vec{q}-\vec{q}^0\\ \vec{p}-\vec{p}^0\end{pmatrix}. \quad (44)$$

Each of the submatrices has a 5×5 or 4×4 dimension. $\underset{\sim}{B}$ is a matrix constructed with the second derivatives of the effective potential energy with respect to the coordinates. $\underset{\sim}{M}$ is the matrix 6×6 obtained from the kinetic energy as a quadratic form of the velocities, $\underset{\sim}{M}^*$ is a 5×5 matrix used to construct the Routh function in terms of the matrix elements of $\underset{\sim}{M}$, $\underset{\sim}{N}^*$ is the inverse matrix of $\underset{\sim}{M}^*$, and $\underset{\sim}{A}$ depends on the vector $\vec{K}$ used to construct $-R$,

$$A_{\mu\nu} = \frac{\partial K_\mu}{\partial q_\nu}, \quad (45)$$

$$B_{\mu\nu} = -\frac{\partial^2}{\partial q_\mu \partial q_\nu}\Big(\frac{(L_z+R_1)^2}{2M_{11}} + V\Big). \quad (46)$$

These quantities are evaluated at the equilibrium position.

The linear stability analysis of the dynamical system (44) consists essentially of finding the eigenvalues (λ) of the 10×10 matrix (8×8 in the rotor case) on the right-hand side, and its eigenvectors $(\vec{V}_q, \vec{V}_p)$. The eigen-values are the (LCE) and represent the exponential shift rate of the coordinates and momenta with respect to their equilibrium values.

The Kelley Theorem says that the tangent space to the phase space at the equilibrium point is generated by the eigenvectors of the matrix of the linearized dynamical system; and that such tangent space is decomposed in subspaces W^s, W^u and W^c (stable, unstable and center) associated respectively with eigenvalues whose real parts are negative, positive and zero. In order to have a hamiltonian dynamical system stable, it is necessary that all the tangent space should be a central manifold.

Figs.3a, 3b

The LCE with positive real part (negative) are associated with the directions along which the phase space point is repelled (attracted) with respect to the equilibrium point. The imaginary part corresponds to rotations around an axis perpendicular to the directions of the attractive or repulsive lines. The eigenvectors are complex and their magnitudes indicate the tangent directions to the trajectory of the motion and their phases determine the motion phases. See the following section.

The eigenvalues and eigenvectors of the matrix $\underset{\sim}{\mathcal{M}}$ were numerically calculated with the help of the Eispack routines. Figures 3 show the real and imaginary parts of the LCE for different values of the magnetic field intensity, in the top equilibrium. There is only one LCE with positive real part.

At the electronic rotor equilibrium the β coordinate is a constant, for this reason two of the LCE are zero, the same value of $det\ \underset{\sim}{M}^{*}$, thus it is necessary to reduce the dimension of the problem from 10 to 8 in this case.

The eigenvectors have ten (eight) complex components, representing the "modes" of the linearized motion in the neighborhood of equilibrium. As in the zero field case (Holle *et al* 1988, Klar 1987a,b), it is found that in the presence of a field, for "most" of the values of the magnetic field intensity, and small values of the angular momentum, the hyperradial coordinate is located in a subspace of the phase space whose Liapunov exponents have real part equal to zero. For these values of H the hyperradial motion is in a subspace with pure imaginary LCE. For this reason, the hyperradius, which is the only coordinate able to describe a fragmentation of the atom, is stable in the linear approximation in the two equilibrium states we have found, for "most of the combinations of L_z and H". The Liapunov exponents with real part different from zero are associated with subspaces containing the hyperspherical coordinates ψ and ϕ. As such coordinates describe the radial and angular correlations (Klar 1987b), it is concluded that there is no linear stability for these correlations. But the linear stability of the hyperradius does not imply that the atom as a whole is stable, since the unstable coordinates, which in the linear approximation are not coupled with the hyperradius, in the exact problem are not linearly coupled with it, giving place to the instability of the atom as a whole. This means that the equilibrium motion, for a relatively long time ($\gg 1/\omega$), decays and the system makes a transition from an almost quasi-periodical motion to a highly aperiodical motion, presumably chaotic before ionization (Berry 1983). The quantum analog of these classical modes of motion is expected to correspond with long living resonances, since before various authors had verified a correspondence between the unstable classical orbits and the metastable states (Miller 1972), and in the hydrogenoid atom in presence of a magnetic field a correspondence between the unstable classical orbits and the quasi-Landau modulations of the photoabsortion cross section of the diamagnetic Rydberg states was verified (Fliedrich and Wintgen 1987).

The energy scales as $H^{2/3}$ and the angular momentum as $H^{-1/3}$ when the length is scaled as $H^{-2/3}$ and the time as H^{-1} (Wintgen and Friedrich 1987). That is, $r = H^{-2/3}\rho$, $E = H^{2/3}\epsilon$, $L_z = H^{-1/3}\lambda$, with which $\rho^4 + 2b\,\rho/a - \lambda^2/(4a^2)$ is obtained for the equilibrium equation and $\epsilon = a\,\rho_0^2 - b/\rho_0 + \lambda/2$ for the scaled energy. See (61) and (62).

Figs.4a,4b,4c,4d,4e

Figs.5a,5b,5c,5d,5e

Figs.6a,6b,6c,6d

Figs.7a,7b,7c,7d

To specify the meaning of "most of the combinations of L_z and H" it is useful to describe the system using the scaled variables. It can be shown that the LCE scale proportionally to H. Then the calculation of the scaled LCE as function of the scaled angular momentum gives a broader description of the stability for different values of H and L_z. Now, as shown in Figures 4-7, the LCE present more drastic changes as function of the scaled angular momentum. The same behavior is shown for the components of the eigenvectors. For the stability analysis it is not sufficient to find the values of scaled L_z for which there are Liapunov exponents with non-zero real part; it is necessary to analyze the components of the eigenvectors along the hyperradial variables r and p_r. There exists "stability", in the before mentioned sense, when there are no real Liapunov and non-zero components of the eigenvectors along r or p_r at the same time. In the top case a qualitative description of this fact is obtained from the expression,

$$\sum_{k=1}^{10} \left(|V_r^{(k)}\, \mathrm{real}\,(\lambda^{(k)})| + |V_{p_r}^{(k)}\, \mathrm{real}\,(\lambda^{(k)})| \right), \tag{47}$$

with a similar expression for the rotor case. When expression (47) is different from zero there is instability in the mentioned sense.

Figures 8 show that there are some small "windows of instability" for the linearized hyperradial motion in the two cases considered. Also it is interesting to mention that there are no such "windows" in the two cases for which the velocity of the hyperradial motion is zero. The "velocity" curves, in Figures 8. were obtained from the expression

$$\sum_{k=1}^{10} \left(|V_r^{(k)} \lambda^{(k)}| + |V_{p_r}^{(k)} \lambda^{(k)}| \right). \tag{48}$$

Figs.8a,8b,8c,8d

6. Quasi-Landau Resonances and Magnetic Susceptibility in One and Two-electron Atoms

The procedure followed in the two-electron atom is more simply applied to the rotating one-electron atom in presence of a magnetic field. In this case we will use spherical coordinates to represent the electron position with respect to an space coordinate system. We will choose the rotating coordinates in such a way that with they the electron position is $(x, 0, 0)$.

The Lagrangian and the angular momentum are

$$L = \frac{1}{2}\dot{r}^2 + \frac{1}{2} r^2 \dot{\theta}^2 + \frac{1}{2} r^2 \sin^2\theta + \frac{Z}{r} - \frac{1}{2} H^2 r^2 \sin^2\theta \dot{\phi}, \tag{49}$$

$$L_z = r^2 \sin^2\theta (\dot{\phi} - \frac{1}{2} H). \tag{50}$$

The ϕ coordinate is cyclic, so the Routh function in the reduced phase space is

$$-R = \frac{1}{2}\dot{r}^2 + \frac{1}{2} r^2 \dot{\theta}^2 + \frac{L_z^2}{2 r^2 \sin^2\theta} + \frac{Z}{r} + \frac{1}{8} H^2 r^2 \sin^2\theta + \frac{1}{2} H L_z, \tag{51}$$

The Hamiltonian in the reduced space of momenta is

$$Q(q,p) = \frac{p_r^2}{2} + \frac{p_\theta^2}{2 r^2} + \frac{L_z^2}{2 r^2 \sin^2\theta} - \frac{Z}{r} + \frac{1}{8} H^2 r^2 \sin^2\theta + \frac{1}{2} H L_z, \tag{52}$$

which has the following minimal points of the potential energy surface $Q(q,0)$ in the 4-dimensional reduced momentum space,

$$p_r = 0, \quad H^2 r^4 + 4 Z r - 4 L_z^2 = 0, \quad p_\theta = 0, \quad \theta = \frac{\pi}{2}, \tag{53}$$

and the following expression for the energy at equilibrium,

$$E = \frac{L_z^2}{2 r^2} - \frac{Z}{r} + \frac{1}{8} H^2 r^2 + \frac{H L_z}{2}. \tag{54}$$

The matrix $\underset{\sim}{\mathcal{M}}$ for the linearized Hamiltonian around the equilibrium position in the phase space, expressed in the coordinates $(r, p_r, \theta, p_\theta)$, is

$$\underset{\sim}{\mathcal{M}} = \begin{pmatrix} 0 & 1 & 0 & 0 \\ \frac{3 r Z - 4 L_z^2}{r^4} & 0 & 0 & 0 \\ 0 & 0 & 0 & \frac{1}{r^2} \\ 0 & 0 & -\frac{Z}{r} & 0 \end{pmatrix}. \tag{55}$$

All the eigen-values are purely imaginary, giving evidence of the linear stability of the system

$$-i\omega_r, \quad i\omega_r, \quad -i\omega_\theta, \quad i\omega_\theta. \tag{56}$$

The eigen-vectors are the columns of the following matrix

$$\begin{pmatrix} 1 & 1 & 0 & 0 \\ 0 & 0 & 0 & 0 \\ i\frac{\omega_r}{2} & -i\frac{\omega_r}{2} & 1 & 1 \\ 0 & 0 & i r^2 \omega_\theta & -i r^2 \omega_\theta \end{pmatrix}. \tag{57}$$

where

$$\omega_r = \frac{(-3 r Z + 4 L_z^2)^{1/2}}{r^2}, \quad \omega_\theta = \left(\frac{Z}{r^3}\right)^{1/2}. \tag{58}$$

This means near the fixed point there is an oscillatory motion, with the semiclassical energy levels of the form

$$E_{n_r, n_\theta} = (n_r + \frac{1}{2})\omega_r + (n_\theta + \frac{1}{2})\omega_\theta. \tag{59}$$

It can be easily shown that these frequencies scale as H.

The states in the neighborhood of the equilibrium have two principal quantum numbers, n_r and n_θ, besides the magnetic quantum number L_z. There are two types of intervals in the spectral lines, with lengths ω_r and ω_θ. For small fields it is satisfied that $r \approx L_z^2/Z$, where $\omega_r \approx \omega_\theta \approx Z^2/L_z^3$, so there exists degeneracy in the motion since the unfolding due to the diamagnetic interaction is of the order of H^2. For high fields, $r \approx (2L_z/H)^{1/2}$, with which $\omega_r \approx H + \mathcal{O}(H^{1/2})$ and $\omega_\theta \approx H^{3/4}$. When $H \to \infty$ it is obtained that $\omega_\theta \ll \omega_r$, with which the interval between spectral lines is $\Delta E \approx H$. This is the interval in the neighborhood of the equilibrium for high fields.

For the equilibria located in the neighborhood of the ionization threshold, we will see that $r = 8L_z^2/9Z$ and $H = 27Z^2/32L_z^3$, reason for which

$$\omega_r = \sqrt{3}\,H, \qquad \omega_\theta = \sqrt{2}\,H. \tag{60}$$

There are two kinds of lines, with intervals given by $1.73\,H$ and $1.41\,H$, relation valid at the threshold. This value is compared with the interval of the quasi-Landau resonances for hydrogen in the presence of a magnetic field reported by various authors (Delande *et al* 1984, Gallas and O'Connell 1982), with the accepted value of $\Delta E = 1.5\,H$.

The two studied cases in the two electron-atom and in the one-electron atom are adapted to the following general formulas, where the symbol "r" means respectively the hyperradius ($\sqrt{2}$ times the gyration radius) and the radius, at equilibrium.

$$E = a\,H^2 r^2 - \frac{b}{r} + \frac{H L_z}{2}, \tag{61}$$

$$H^2 r^4 + \frac{2\,b\,r}{a} - \frac{L_z^2}{4\,a^2} = 0, \tag{62}$$

where the constants a and b have the following expressions

$$a = \begin{cases} \dfrac{1}{4}, & \text{one-electron atom;} \\ \dfrac{1}{4}, & \text{rotor;} \\ \dfrac{k^2}{4}, & \text{top;} \end{cases} \qquad b = \begin{cases} \dfrac{Z}{2}, & \text{one-electron atom;} \\ \dfrac{4\,Z-1}{2^{3/2}}, & \text{rotor;} \\ Z\,k^2\,2^{1/2}, & \text{top.} \end{cases} \tag{63}$$

The quantity k in the top case is related to the value of the mock angle ψ at equilibrium, equation (33).

It is interesting to analyze the family of curves E vs H for high values of L_z and in the neighborhood of the ionization threshold, $E = 0$. Equations (61) and (62) for the equilibrium and the energy when combined give us the following expressions for the quantities r and H

$$r = \frac{L_z^2}{9\,a\,b}, \qquad H = \frac{27\,a\,b^2}{2\,L_z^3}. \tag{64}$$

From equations (61) and (62), with fixed values of Z, L_z and H is obtained

$$\frac{\partial E}{\partial L_z} = \frac{L_z}{4\,a\,(2\,H^2\,a\,r^3 + b)}, \tag{65}$$

from which, near the threshold we obtain

$$\frac{\partial E}{\partial L_z} = 2\,H. \tag{66}$$

This value can be compared with the interval of the quasi-Landau resonances reported by various authors (Delande *et al* 1984, Gallas and O'Connell 1982), with the accepted value $\Delta E = 1.5\,H$. It is necessary to note that the quasi-Landau resonances do not coincide with the equilibrium states we are considering, since these are characterized to be a series of states with different principal quantum numbers (approximate) associated to each of the values of the angular momentum (in our case L_z). The quantum motion associated with the classical rotating atom at equilibrium with a given value of L_z is the ground state of a series of quasi-Landau resonances. For small values of H it was found (Delande *et al* 1984) that the principal quantum number n is related with the number of nodes N_r of the radial wave function and the magnetic quantum number M through

$$n = N_r + |M| + 1. \tag{67}$$

This can permit us to conjecture that equation (66) effectively gives the quasi-Landau resonances interval. In order to be precise, equation (66) gives us the interval between the ground states of the oscillatory motions corresponding to consecutive values of L_z, and the quasi-Landau resonances would be a set of discrete states associated with each value of L_z.

In the two-electron system, for the equilibria located near the ionization threshold it is true that the hyperradius has the value $r = L_z^2/9ab$ and $H = 27ab^2/2L_z^3$. We can perform an analysis similar to the hydrogenoid case, with several fundamental differences. The effective potential energy surface does not present minima for none of the equilibria, but only saddle points, for this reason there are no stable oscillations around equilibrium, even though there are oscillations during certain time before the system becomes separated from equilibrium. In our case, the problem has a number of frequencies equal to the dimension of the reduced configuration space. In the top case there are five frequencies and in the rotor case only four. Then there are several intervals for the quasi-Landau resonances. As the system is unstable, some of the frequencies are imaginary. The frequencies are merely the Liapunov exponents of the linearized motion around the equilibrium corresponding to zero energy. Another difference with the hydrogenoid case, which is separable in the linear approximation, is the unstable oscillations occurring on planes of the reduced phase space which do not necessarily coincide with the phase space planes $(q_\mu - p_\mu)$, and for this reason the indexes in the frequencies do not necessarily coincide with the coordinate names. In the hydrogenoid case, there are regular and chaotic bound motions, and there are KAM surfaces in the phase space enclosing the chaotic orbits, but in our case there are no KAM surfaces and every instability leads necessarily to dissociation of the system, which is now

faster than simple Arnold diffusion. The orbits we have obtained are unstable, but in the hydrogenoid case, there are stable and unstable orbits. In the hydrogenoid case, the system is integrable in the two extreme cases, $H \to 0$ and $H \to \infty$, with a different behaviour in our case.

In the top case the frequencies (pure imaginary LCE) at threshold are

$$\omega_1 = 1.54609\,H, \qquad \omega_2 = 1.19798\,H, \qquad \omega_3 = 2.75043\,H, \qquad \omega_4 = 0.90345\,H, \tag{68}$$

and the exponential divergence constant (absolute value of the real part of four of the LCE) is

$$\lambda = 1.2294\,H. \tag{69}$$

The eigenvectors associated with the two LCE with real part have the form

$$\begin{pmatrix} 1-0.03i \\ 0.109+0.003i \\ -1.822+1.2i \\ -1.132-0.026i \\ 0 \\ 0 \\ 0 \\ 0 \\ 3.021-2.857i \\ -0.569+0.071i \end{pmatrix}; \qquad \begin{pmatrix} 1-3.052i \\ -0.091+0.339i \\ 5.345-4.522i \\ -0.945+3.51i \\ 0 \\ 0 \\ 0 \\ 0 \\ -11.536+6.713i \\ -0.734+1.688i \end{pmatrix}, \tag{70}$$

where the columns are numbered with the scheme (β, p_β), ... (ϕ, p_ϕ). It is observed that, as we have said when presenting the stability analysis, the instability affects firstly the phase planes (β, p_β), (γ, p_γ) and (ϕ, p_ϕ). The planes (r, p_r) and (ψ, p_ψ) are stable in the linear approximation.

In the rotor case the β coordinate does not appear and besides when $\beta = \pi/2$, the problem can be completely separated in the linear approximation. The frequencies (purely imaginary LCE) at threshold are

$$\omega_\gamma = 1.41421\,H, \qquad \omega_r = 1.73205\,H. \qquad \omega_\psi = 1.63299\,H \tag{71}$$

and the exponential divergence constant (absolute value of the real part of two of the LCE) is

$$\lambda_\phi = 2.70801\,H. \tag{72}$$

The eigenvectors associated with these LCE have elements different from zero in the corresponding phase planes, when $\beta = \pi/2$.

There are 7 classes of lines, with intervals $1.73\,H$, $1.41\,H$, $1.63\,H$, $1.54\,H$, $1.19\,H$, $2.75\,H$ and $0.9\,H$, at threshold. These values are compared with the quasi-Landau resonances interval experimentally found in atoms with one excited electron under the presence of a magnetic field reported by various authors (Delande *et al* 1984, Gallas and O'Connell 1982), with the accepted value $\Delta E = 1.5\,H$. It is expected that the time life of these states oscillates between $1/(2.7\,H)$ and $1/(1.2\,H)$

The magnetic susceptibility of the motions at equilibrium can easily be calculated from the expressions for energy. The general result, valid for the hydrogenoid atom and for the rotor and top states in atoms with two excited electrons, is the following

$$\mu = \frac{\partial^2 E}{\partial H^2} = \frac{b\,r^2}{2\,H^2 r^3 + \dfrac{b}{a}}. \tag{73}$$

When $H = 0$, this formula gives us in each of the mentioned cases a formula for the magnetic susceptibility of the lower states between each of the states associated with each of the L_z values, respectively,

$$\mu_{|H=0} = \frac{L_z^4}{4\,Z^2}, \qquad \frac{L_z^4}{2(4\,Z-1)^2}, \qquad \frac{L_z^4}{32\,Z^2\,k^6}. \tag{74}$$

(see Figures 9).

Figs.9a,9b

7. Concluding remarks

There exist two kinds of rotational motions at equilibrium in the double highly excited states of two-electron atoms in the presence of a magnetic field. These states can exist during a relatively long time before ionization. The hyperradial coordinate is stable in the linear approximation, on some "windows" of stability in the scaled angular momentum parameter. However, the hyperradial coordinate is not an adiabatic variable; then, quantum solutions describing, in their classical limit, a rotating rigid body must consist of a superposition of adiabatic channels. The effect of the field is to reduce the atomic size without changing its shape, and to change the angular frequency of the rotation, without altering the radial and angular correlations. The studied resonances are located above those corresponding to the free case. When the angular momentum grows, the resonances are located in higher regions of the spectrum and the distance among them is higher. It is found that threshold values for the magnetic field intensity which separate the spectrum in bound and ionizing do not exist, however the analysis of the scaled LCE shows that for some combinations of H and L_z the system presents higher instability in the hyperradial motion. The classical values of the magnetic susceptibilities and the quasi-Landau resonances interval would be compared with experimental measurements on Rydberg states in the presence of a magnetic field.

ACKNOWLEDGMENTS

The author is grateful to Dr. P. Grujić for useful discussions and suggestions. He would also like to thank Professor Abdus Salam, the International Atomic Energy Agency and UNESCO for hospitality at the International Centre for Theoretical Physics, Trieste. The Centro de Investigaciones en Ciencias Exactas y Naturales of the Universidade de Antioquia is acknowledged for financial support and encouragement.

References

Abraham R and Marsden J E 1978 *Foundations of Mechanics* 2nd ed (Reading: Benjamin)

Berry M 1983 *Chaotic Behavior of Deterministic Systems* Les Houches Session XXXVI eds G Iooss, R H G Helleman and R Stora (Amsterdam: North Holland) 171-272

Delande D, Biraben F and Gay J C 1984 *New Trends in Atomic Physics* Les Houches Session XXXVIII eds G Grynberg and R Stora (Amsterdam: Elsevier) 352-380

Delos J B, Knudson S K and Noid D W 1983 *Phys. Rev. A* **28** 7-21

—— 1984 *Phys. Rev. A* **30** 1208-1218

Dimitrijević M S and Grujić P V 1984 *Z. Naturforsch* **39a** 930-938

Fano U 1983 *Rep. Prog. Phys.* **46** 97-165

Fock V K 1958 *Nor. Vidensk. Selsk. Forh.* **31** 138-151

Friedrich H and Wintgen D 1989 *Phys. Rep.* **183**, 37-39

Gallas J A C and O'Connell R F 1982 *J. Phys. B: At. Mol. Phys.* **15**L75-L80

Holle A, Main J, Wiebusch G, Rottke H and Welge K H 1988 *Phys. Rev. Lett.* **61** 161-164

Klar H 1985 *J. Math. Phys.* **26** 1621-1625

—— 1986a *Few Body Systems* **1** 123-144

—— 1986b *Z. Phys.* **D6** 353-358

—— 1986c *Phys. Rev. Lett.* **57** 66-69

—— 1987a *Z. Phys.* **D6** 107-111

—— 1987b *J. Opt. Soc. Am.* **B4** 788-793

Langmuir I 1921 *Phys. Rev.* **17** 339

Mahecha J 1989 *Few Body Systems* **6** 183-192

Miller W H J 1972 *Chem. Phys.* **56** 38-45

Poirier M 1989 *Phys. Rev. A* **40** 3498-3504

Schuster H G 1988 *Deterministic Chaos* (Weinheim: Physik Verlag)

Smith F T 1962 *J. Math. Phys.* **3** 375-748

Wannier G 1953 *Phys. Rev.* **90** 817-825

Whittaker E T 1937 *Analytical Dynamics* 4th ed (Cambridge: Cambridge University Press)

Wintgen D and Friedrich H 1987 *Atomic Diamagnetism* In Physics of Atoms and Molecules ed K T Taylor (New York: Plenum)

Wuner G and Ruder A 1987 *Phys. Scripta* **36** 291-299

FIGURE CAPTIONS

Figure 1. Two-electron atoms with rotation at equilibrium under the presence of a homogeneous magnetic field in the z direction. **(a)** Electronic top. The rotation is phase locked. The orbital radius and the distance between the planes diminishes when the field intensity is increased. The angle θ_{12} does not vary with the field. **(b)** Electronic rotor. The electrons are rotating 180° out of phase along parallel orbits. $\pi/2 - \beta$ is the angle between the interelectronic line and the z axis.

Figure 2. **(a)** Values of the hyperradius at equilibrium for H^- with $L_z = 1, 2, ...5$ for the electronic top. The values for the electronic rotor are similar. **(b)** Is represented the behavior of the scaled hyperradius in the top and rotor cases.

Figure 3. **(a)** Real parts of the ten LCE for the H^- with $L_z = 5$ at the top equilibrium, for different values of H. Only two of LCE have real part different from zero. The corresponding diagram for the rotor is similar. The values of all the LCE decrease when L_z increases. **(b)** The corresponding imaginary parts.

Figure 4 (a), (b), (c), (d), (e). Positive real parts of the scaled LCE for the H^- at the top equilibrium.

Figure 5 (a), (b), (c), (d), (e). Positive imaginary parts of the scaled LCE for the H^- at the top equilibrium.

Figure 6 (a), (b), (c), (d). Positive real parts of the scaled LCE for the H^- at the rotor equilibrium. β is equal to $\pi/2$.

Figure 7 (a), (b), (c), (d). Positive imaginary parts of the scaled LCE for the H^- at the rotor equilibrium. β is equal to $\pi/2$.

Figure 8 (a), (b), (c), (d). Curves qualitatively describing the instabilities of the top and rotor equilibria, obtained from (47), and curves qualitatively describing the behavior of velocity, obtained from (48). Arbitrary units are used. β is equal to $\pi/2$.

Figure 9. **(a)** The energy as a function of the magnetic field intensity for the H^- with $L_z = 1, 2, ...5$ for the electronic top. The electronic rotor curves are similar. **(b)** The scaled energy curves for the two cases are also shown.

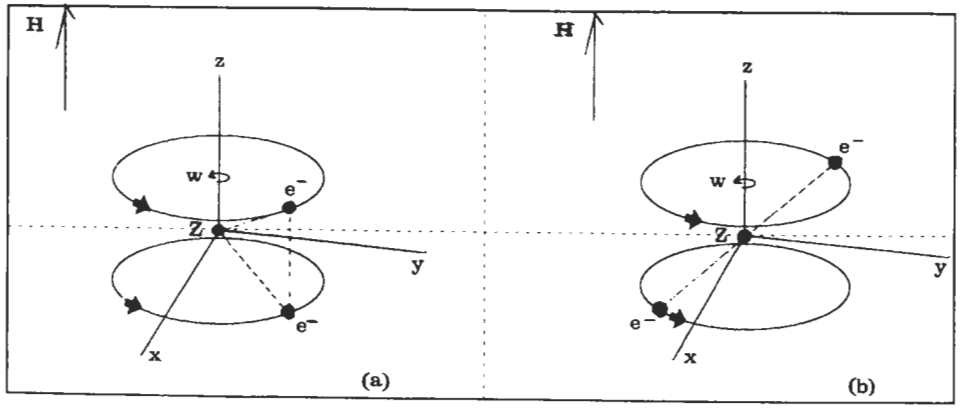

Fig.1

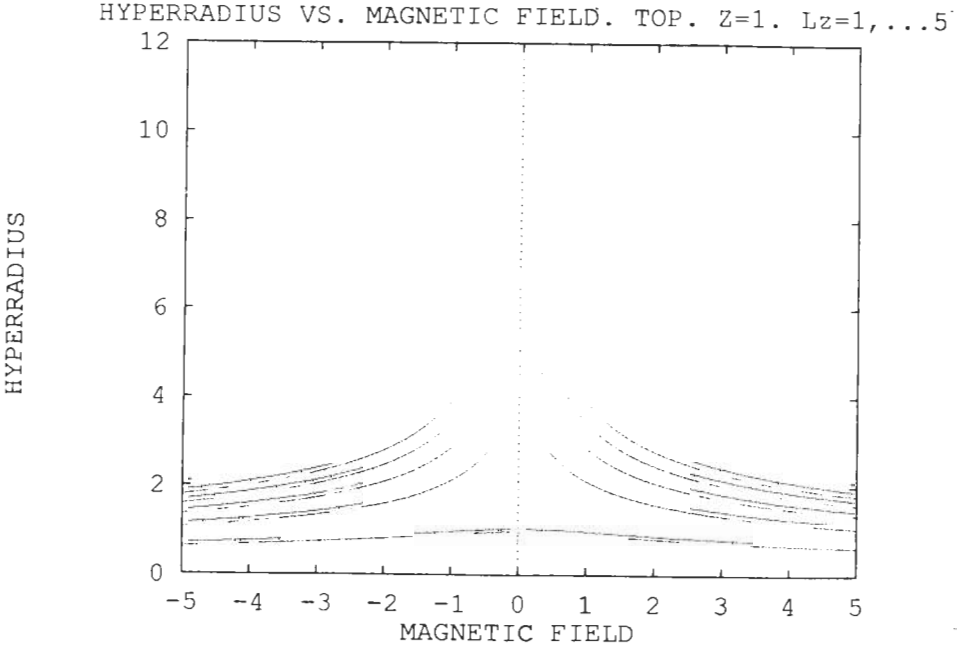

Fig.2a

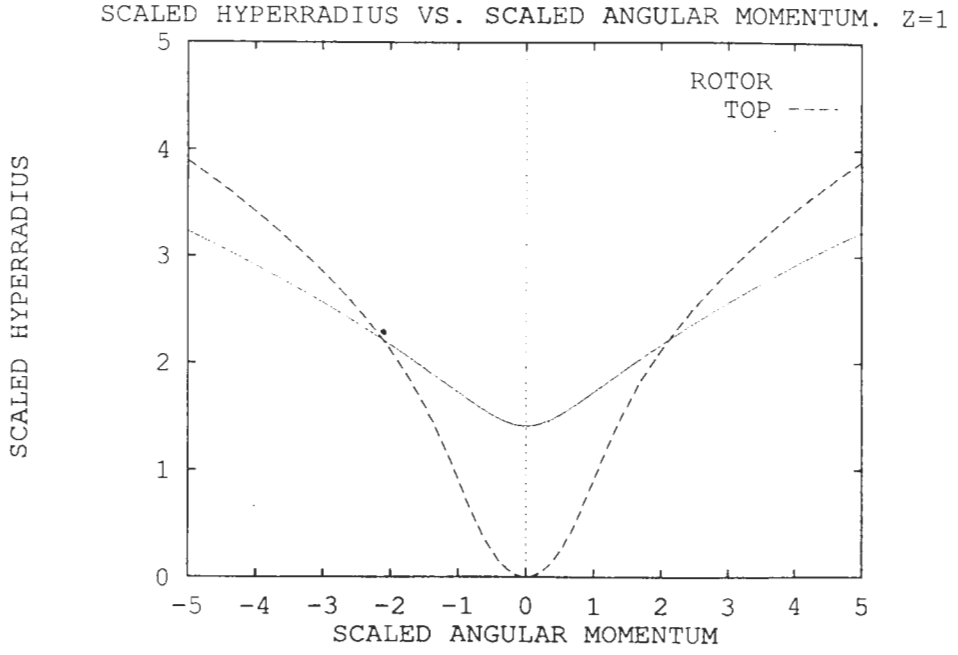

Fig.2b

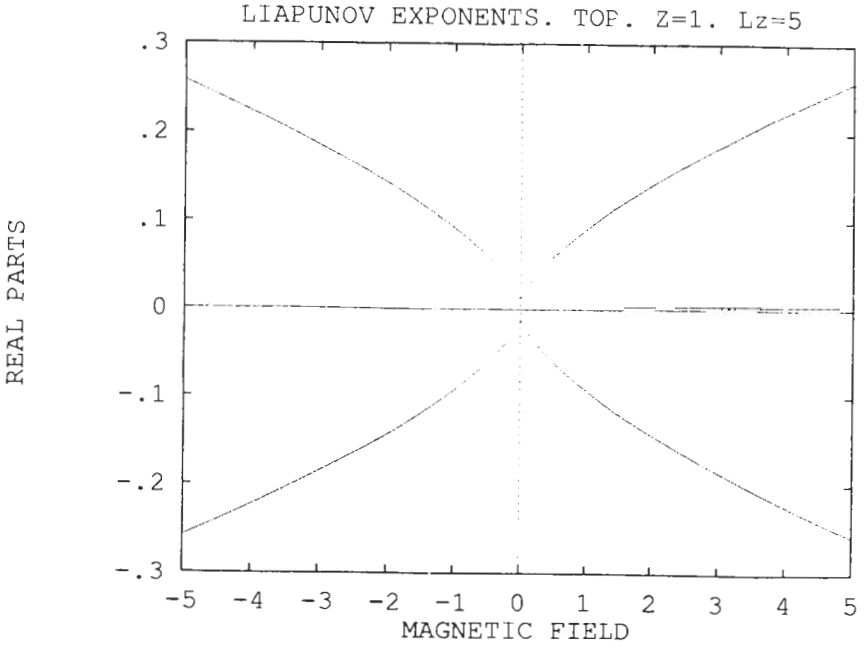

Fig.3a

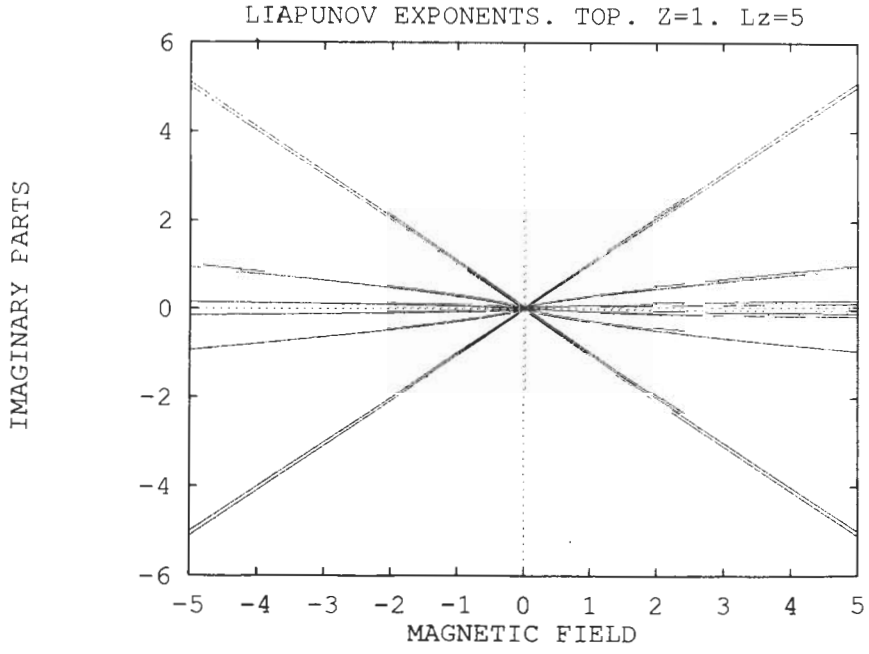

Fig.3b

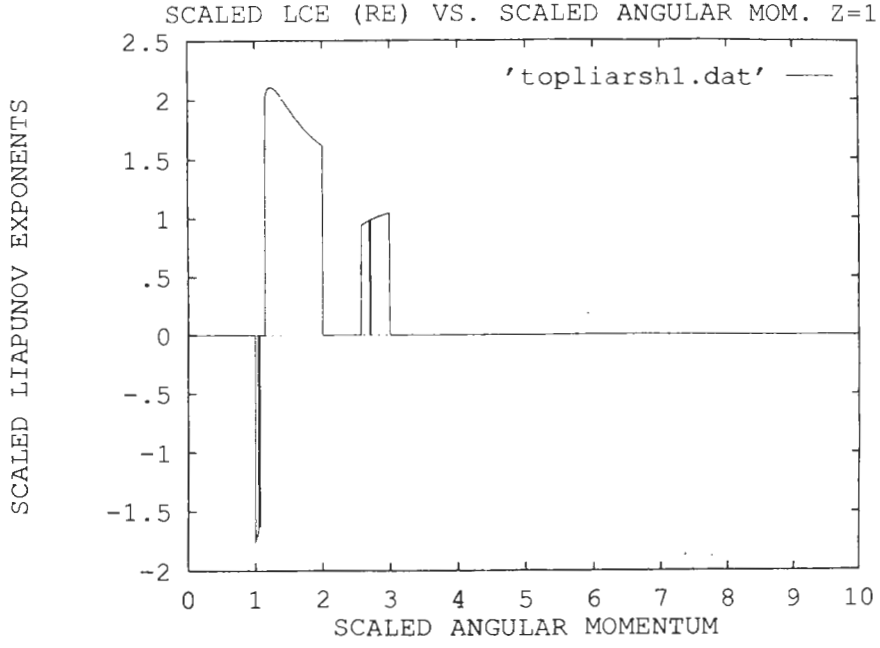

Fig.4a

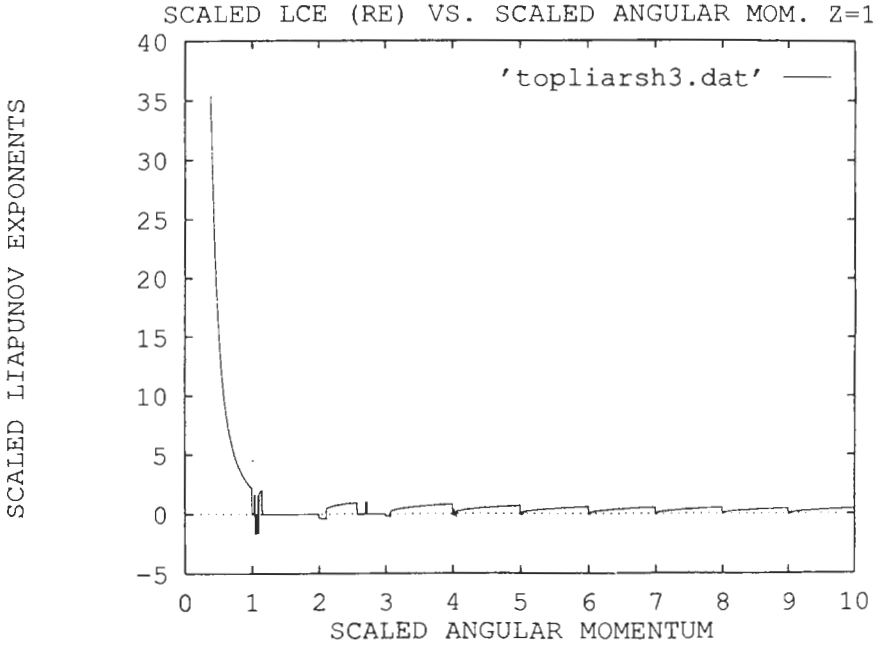

Fig.4b

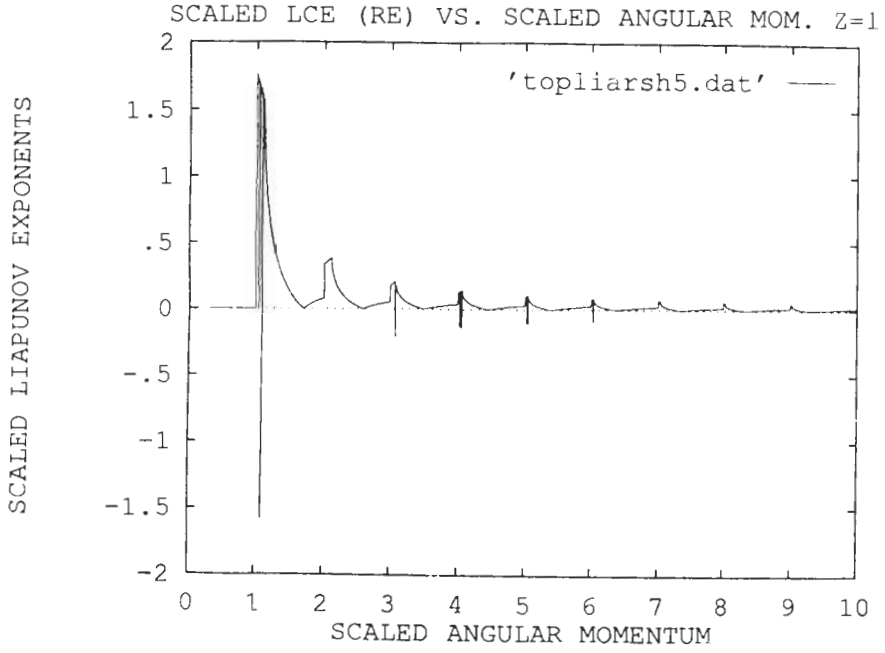

Fig.4c

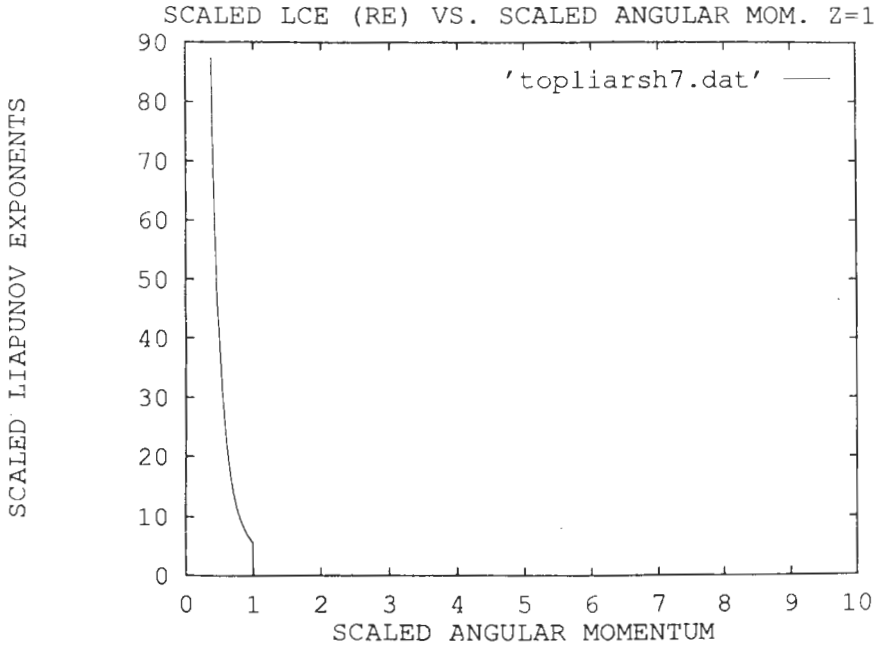

Fig.4d

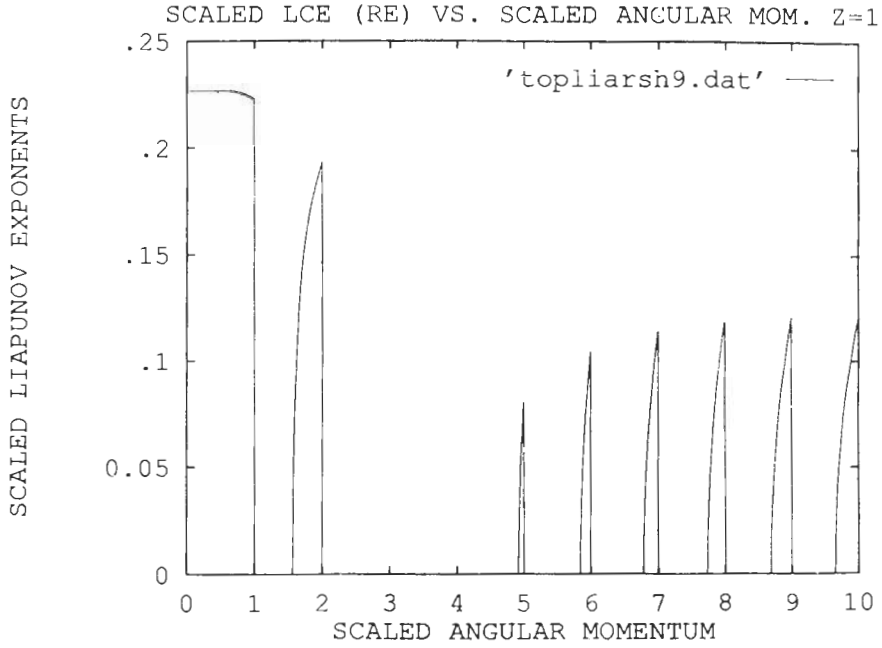

Fig.4e

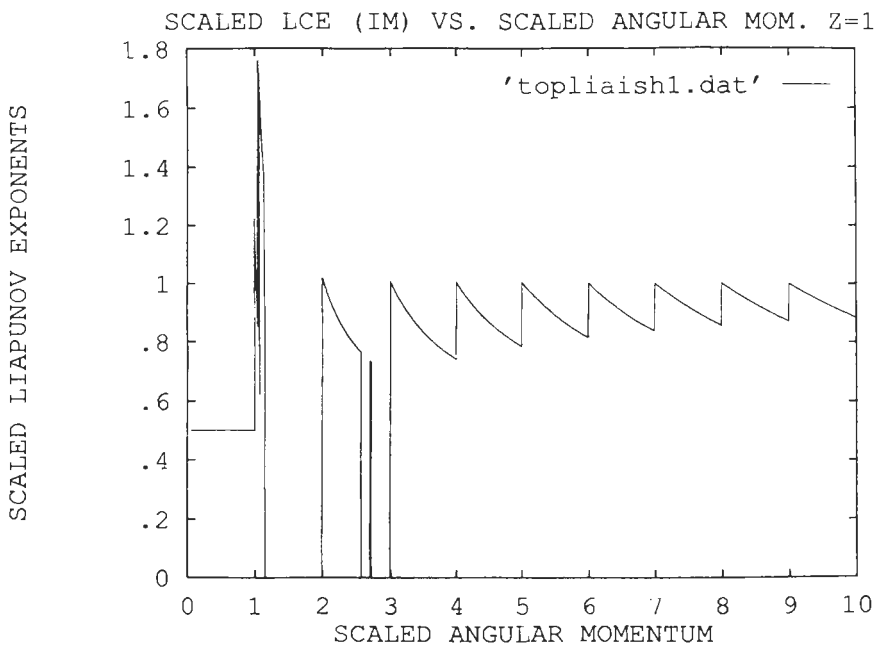

Fig.5a

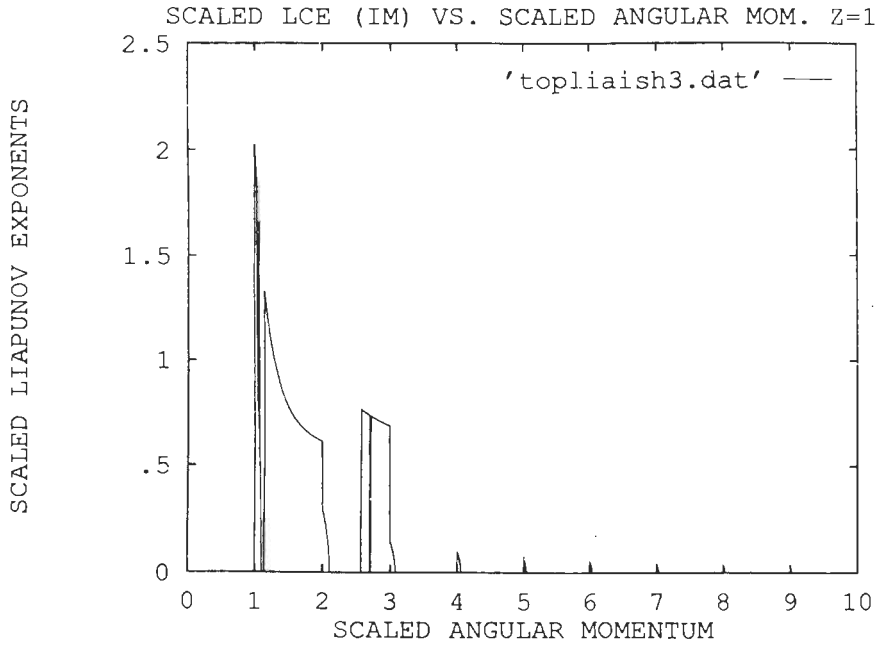

Fig.5b

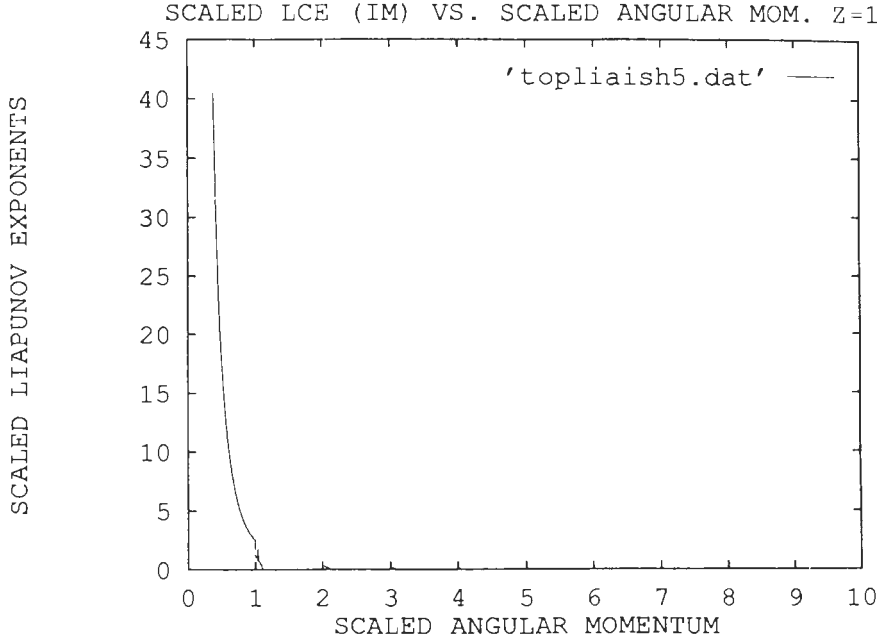

Fig.5c

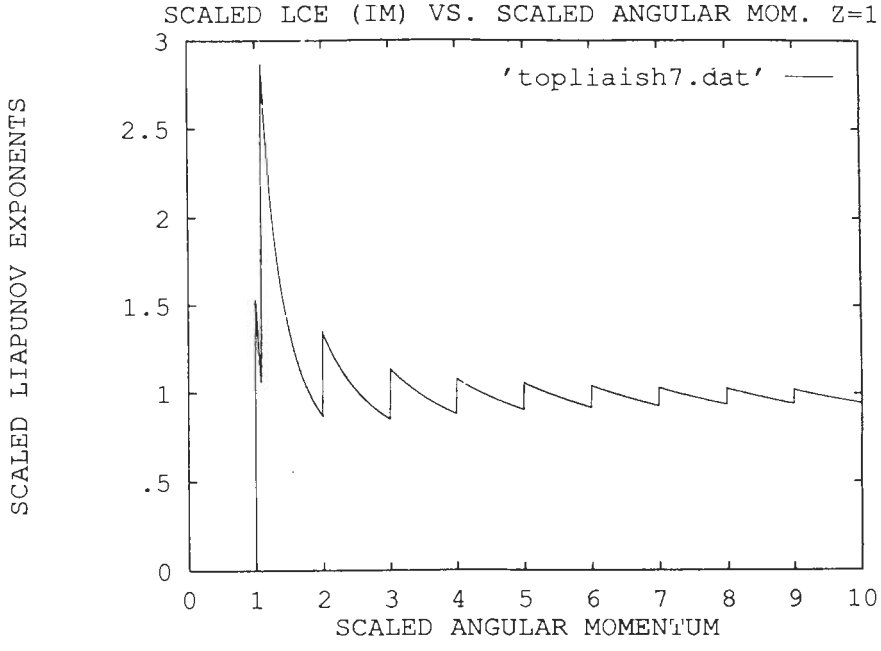

Fig.5d

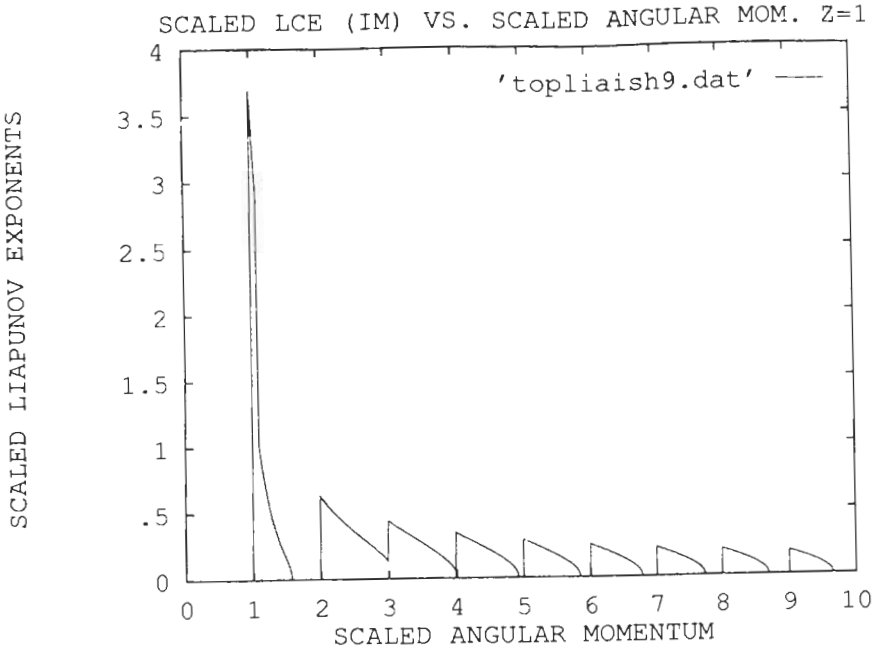

Fig.5e

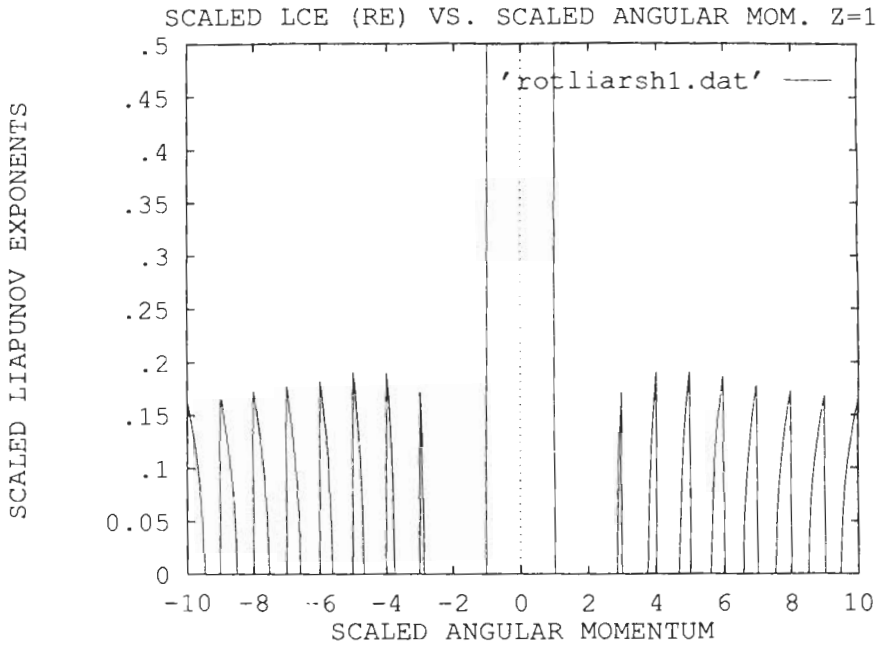

Fig.6a

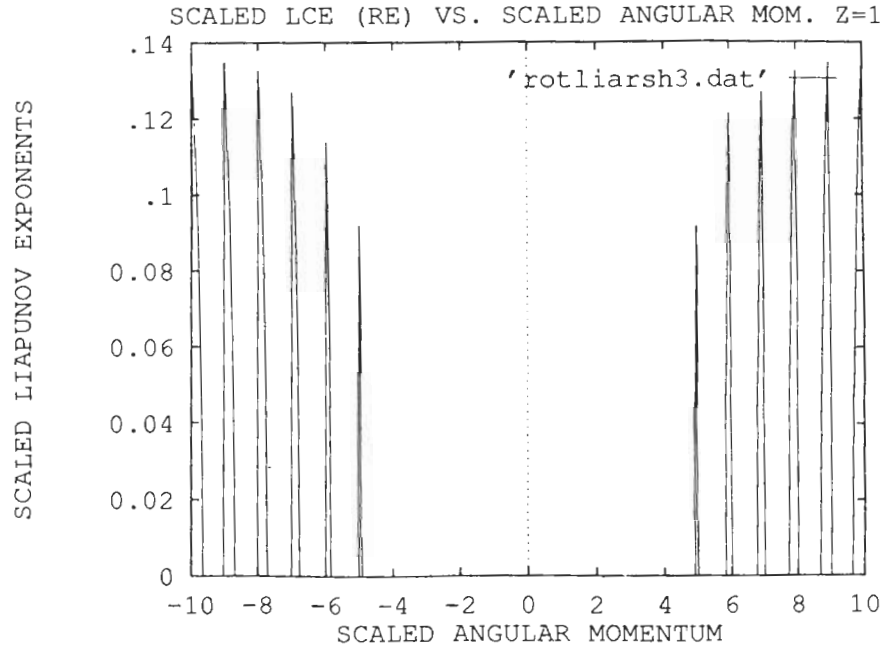

Fig.6b

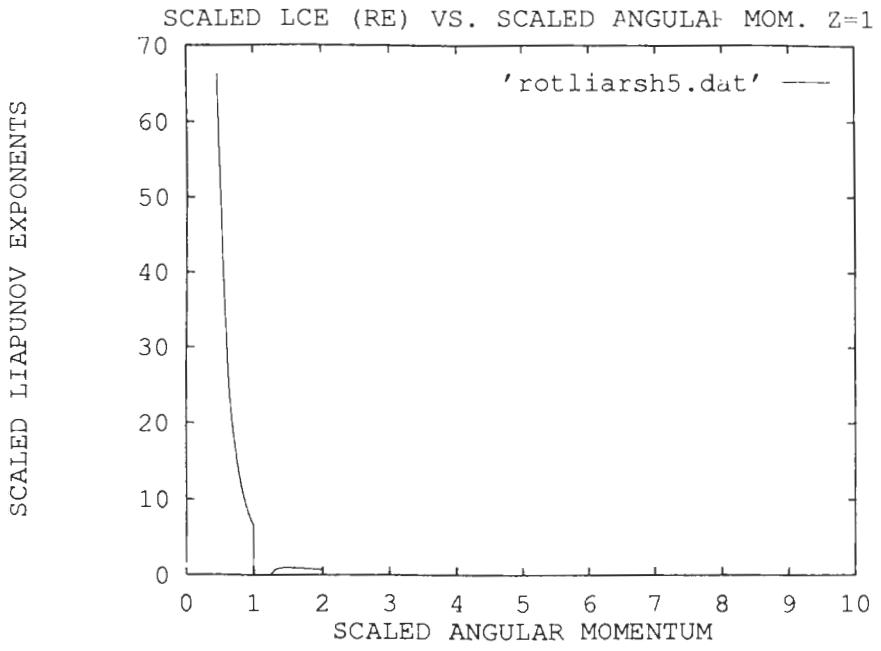

Fig.6c

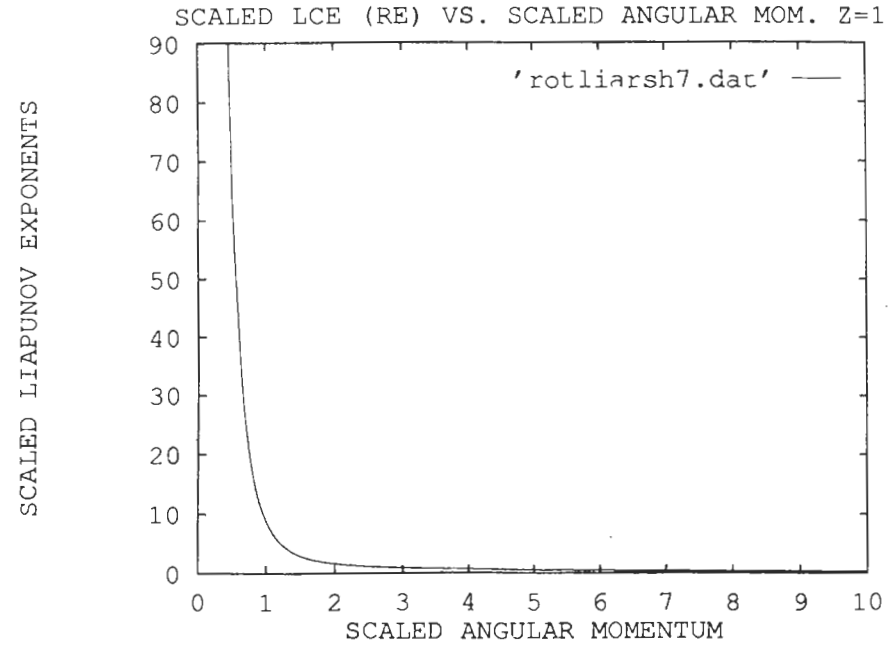

Fig.6d

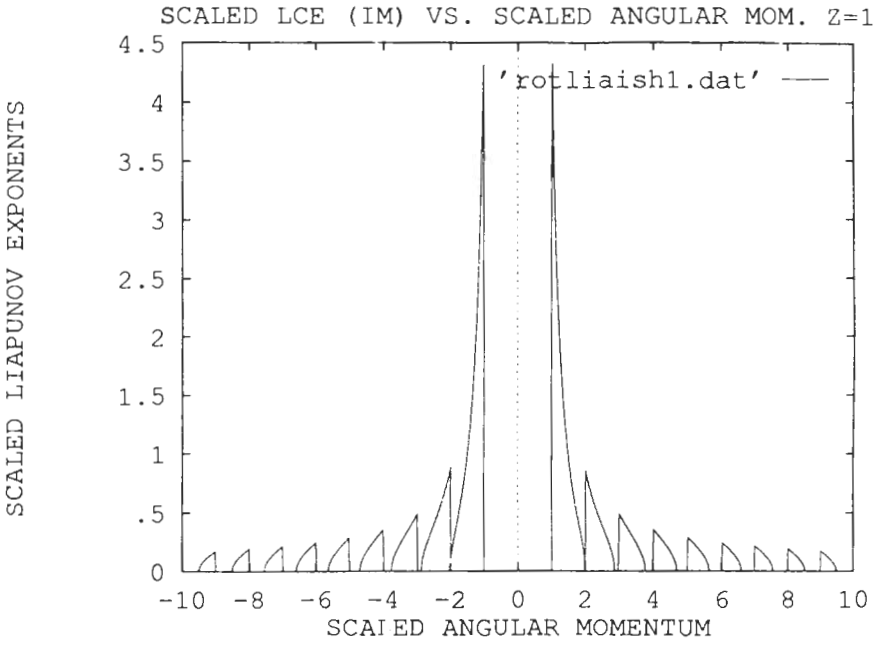

Fig.7a

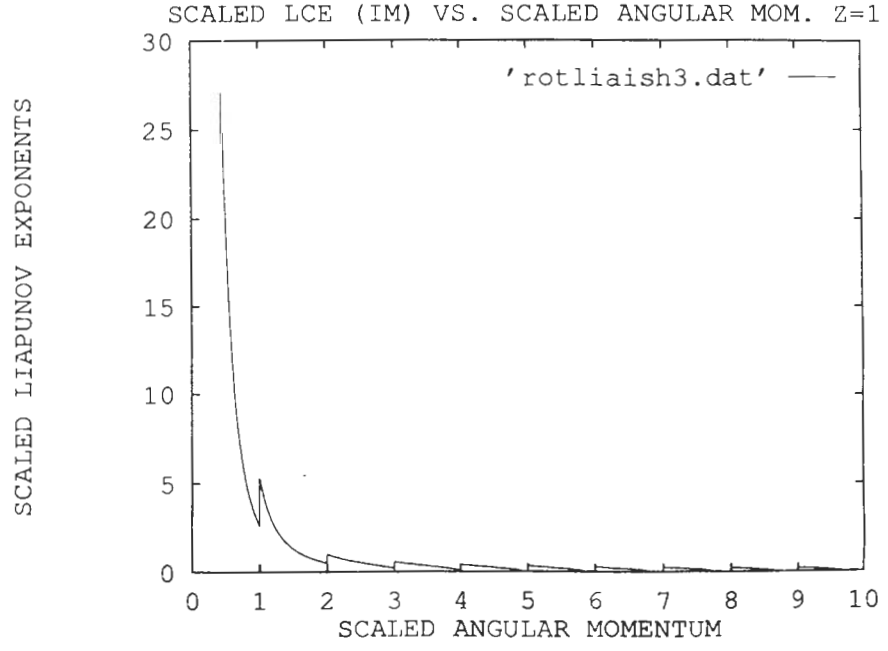

Fig.7b

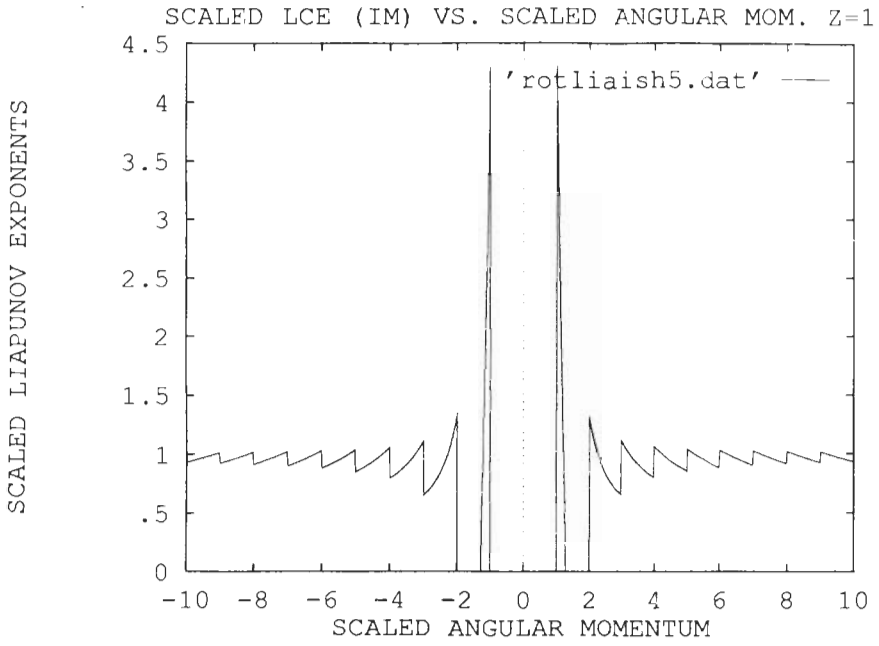

Fig.7c

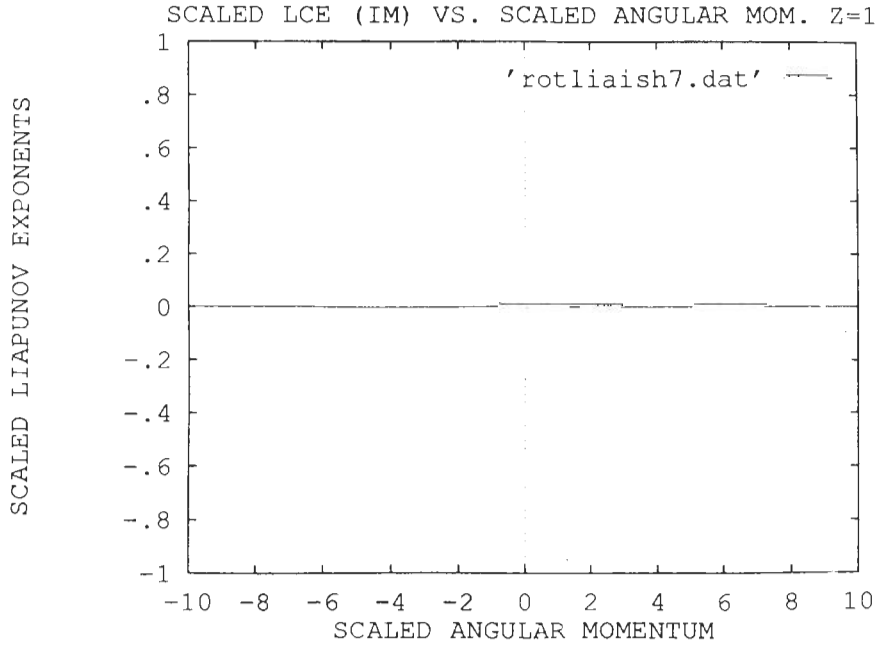

Fig.7d

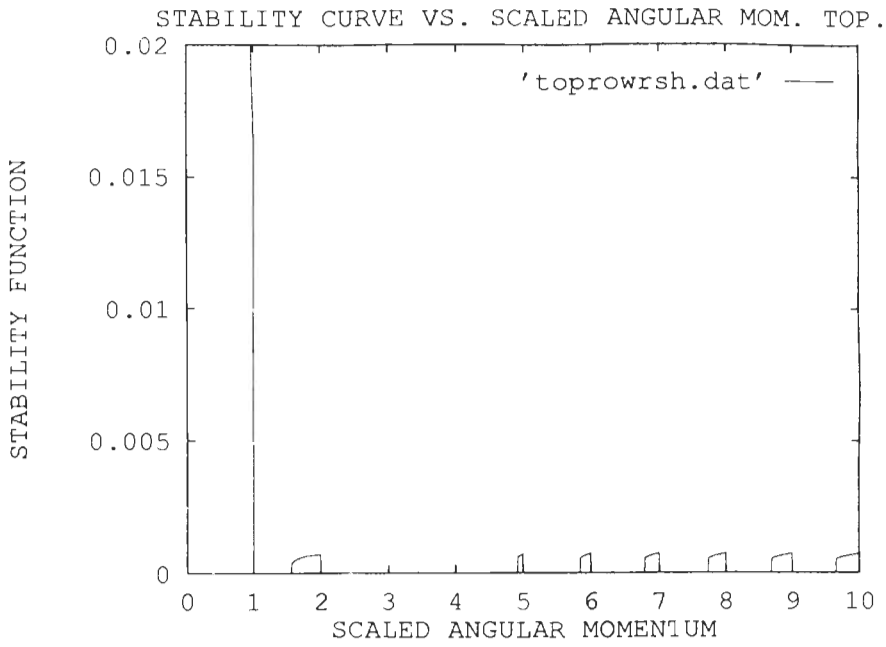

Fig.8a

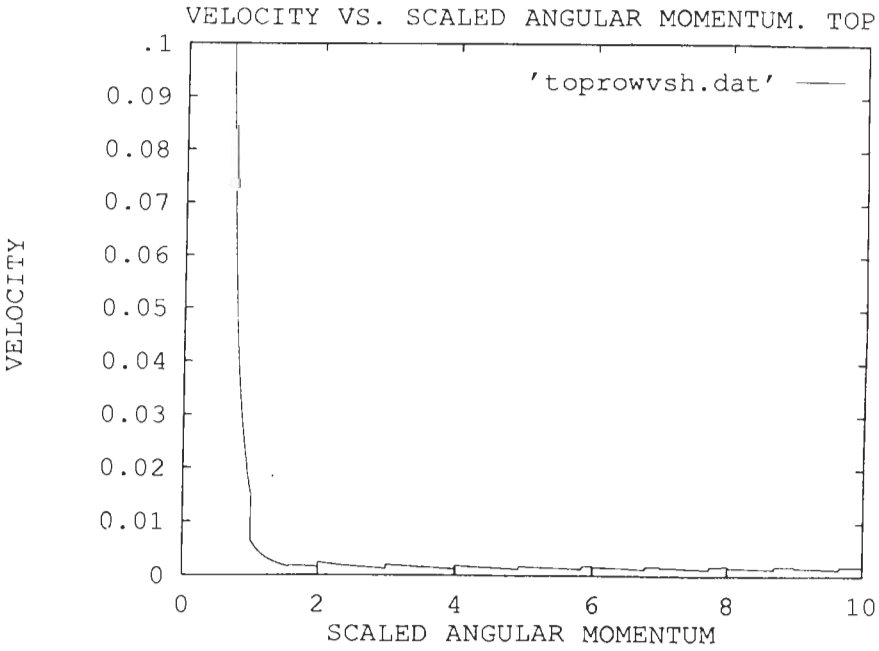

Fig.8b

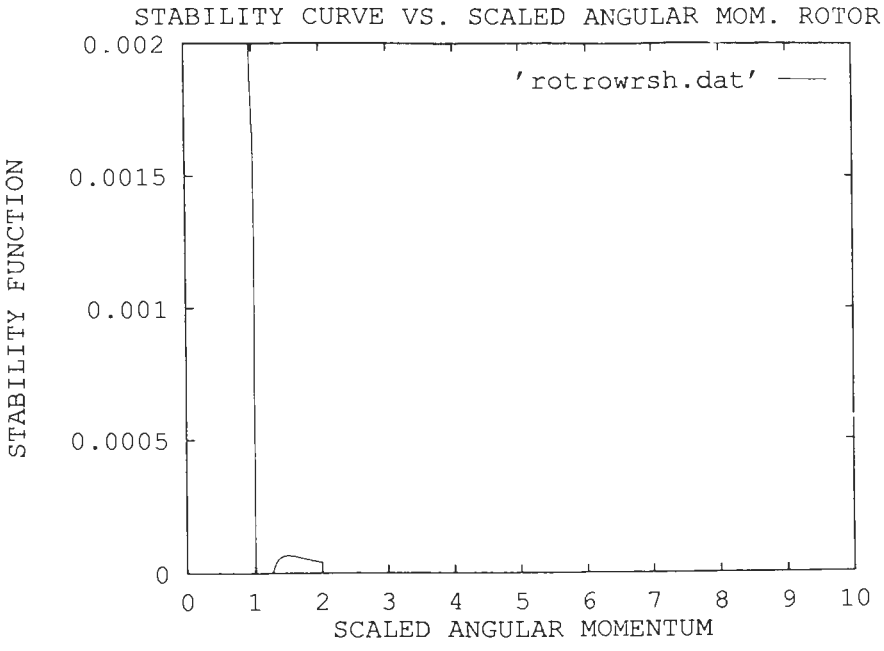

Fig.8c

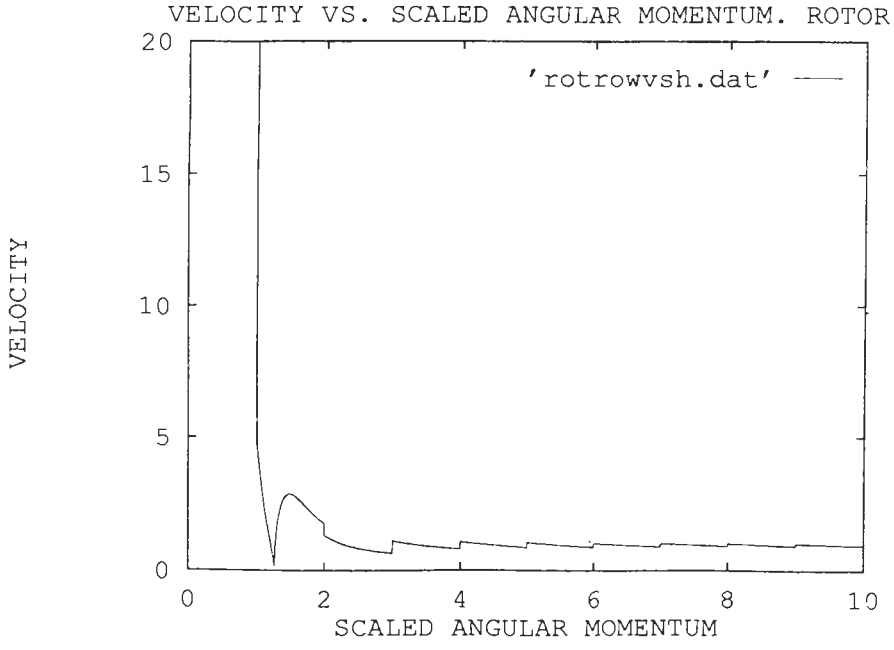

Fig.8d

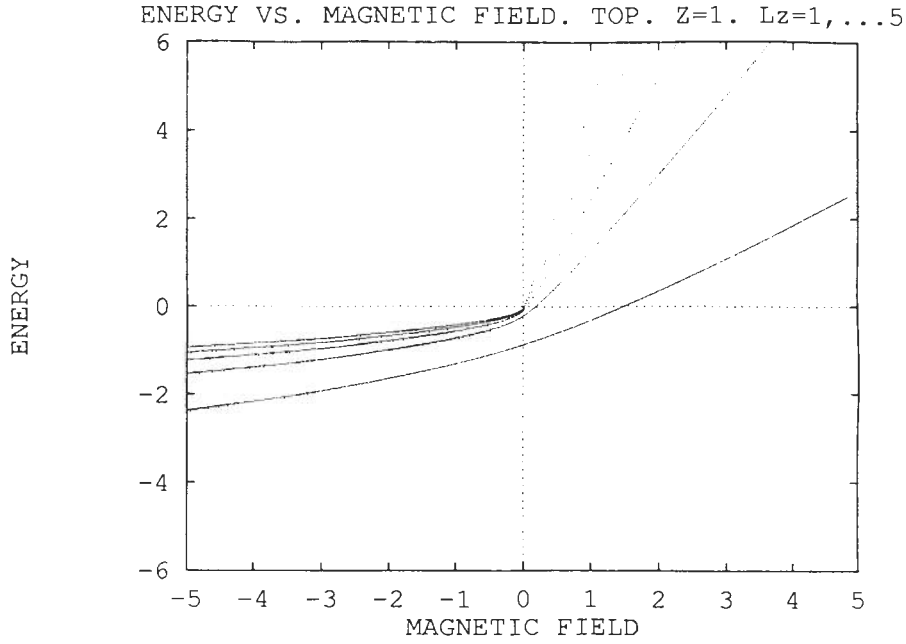

Fig.9a

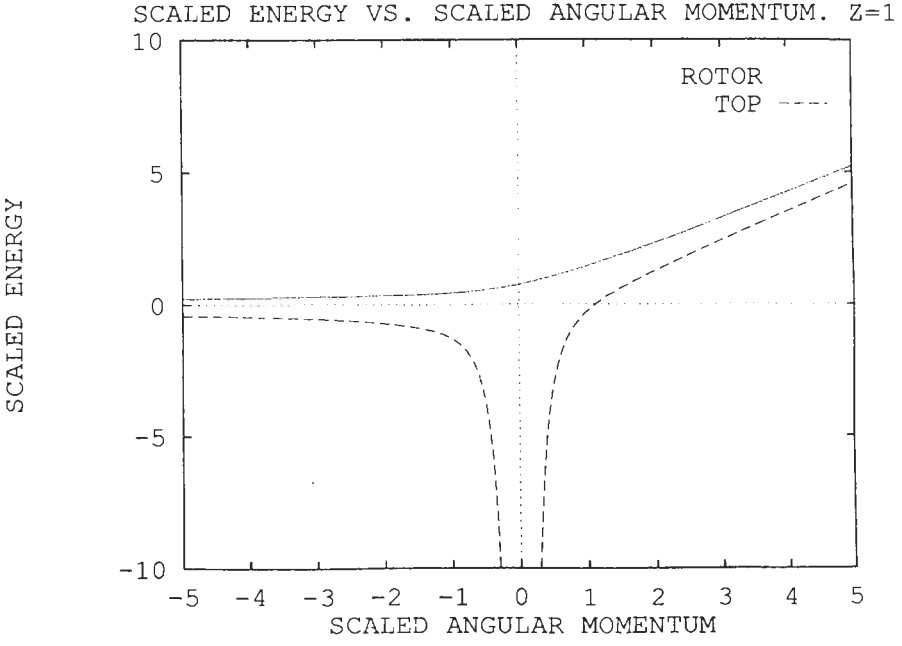

Fig.9b